Semi-Annual Report

Pseudomorphic Semiconducting Heterostructures from Combinations of AlN, GaN and Selected SiC Polytypes: Theoretical Advancement and its Coordination with Experimental Studies of Nucleation, Growth, Characterization and Device Development

Supported under Grant #N00014-90-J-1427
Department of the Navy
Office of the Chief of Naval Research
Report for the period January 1, 1993–June 30, 1993

Robert F. Davis, K. S. Ailey, R. S. Kern,
R. Patterson, S. Tanaka, and C. Wang
Materials Science and Engineering Department
North Carolina State University
Campus Box 7907
Raleigh, NC 27695-7907

June 1993

REPORT DOCUMENTATION PAGE

Form Approved
OMB No. 0704-0188

1. AGENCY USE ONLY *(Leave blank)*	2. REPORT DATE	3. REPORT TYPE AND DATES COVERED
	June, 1993	Semi-Annual 1/1/93–6/30/93

4. TITLE AND SUBTITLE

Pseudomorphic Semiconducting Heterostructures from Combinations of AlN, GaN and Selected SiC Polytypes: Theoretical Advancement and its Coordination with Experimental Studies of Nucleation, Growth, Characterization and Device Development

5. FUNDING NUMBERS

414s007---01
1114SS
N00179
N66005
4B855

6. AUTHOR(S)

Robert F. Davis

7. PERFORMING ORGANIZATION NAME(S) AND ADDRESS(ES)

North Carolina State University
Hillsborough Street
Raleigh, NC 27695

8. PERFORMING ORGANIZATION REPORT NUMBER

N00014-90-J-1427

9. SPONSORING/MONITORING AGENCY NAMES(S) AND ADDRESS(ES)

Sponsoring: ONR, Code 1513:CMB, 800 N. Quincy, Arlington, VA 22217-5000
Monitoring: Office of Naval Research Resider
The Ohio State University Research Center
1960 Kenny Road
Columbus, OH 43210-1063

10. SPONSORING/MONITORING AGENCY REPORT NUMBER

11. SUPPLEMENTARY NOTES

12a. DISTRIBUTION/AVAILABILITY STATEMENT

Approved for Public Release; Distribution Unlimited

12b. DISTRIBUTION CODE

13. ABSTRACT *(Maximum 200 words)*

Solid solutions and pseudomorphic heterostructures of AlN and SiC have been grown on vicinal α(6H)-SiC substrates via plasma-assisted, gas-source molecular beam epitaxy at 1050°C. Reflection high energy electron diffraction, high resolution TEM and Auger depth profiling show the films to be monocrystalline and to possess the desired chemical compositions. The solid solutions have the wurtzite structure. The multilayers have the following phases: α(6H)-SiC substrate, 2H-AlN and 3C-SiC. Chemical interdiffusion between α(6H)-SiC wafers and epitaxially deposited 2H-AlN films are under investigation within the temperature range of 1500°C to 1700°C. Scanning Auger spectroscopy and XTEM is being used to determine the diffusion profiles and the occurrence of new phases. The Auger data and electron energy loss measurements are in disagreement. Additional diffusion and segregation research is under way to resolve this conflict. Superlattices of GaN/AlN on sapphire and SiC have been extensively investigated via HRTEM. Below the critical thickness, AlN only contains threading dislocations emanating from the misfit dislocations; above this thickness, defects parallel to the growth surface greatly increase. Deposition of GaN on sapphire or SiC results in a larger number of threading dislocations caused by the large misfit as well as a high concentration of dislocations parallel to the growth surface. Both types of defects are decreased in density if the GaN is deposited on AlN.

14. SUBJECT TERMS

pseudomorphic structures, 3C-SiC, 6H-SiC, GaN, AlN, gas-source molecular beam epitaxy, chemical interdiffusion, threading dislocations, misfit dislocations, critical thickness

15. NUMBER OF PAGES

30

16. PRICE CODE

17. SECURITY CLASSIFICATION OF REPORT	18. SECURITY CLASSIFICATION OF THIS PAGE	19. SECURITY CLASSIFICATION OF ABSTRACT	20. LIMITATION OF ABSTRACT
UNCLAS	UNCLAS	UNCLAS	SAR

Table of Contents

I.	Introduction	1
II.	Solid Solutions and Pseudomorphic Multilayer Heterostructures in the System AlN-SiC Produced by Plasma-assisted, Gas-source Molecular Beam Epitaxy	2
III.	Determination of the Diffusivity of Si, C, Al and N at the Interface of the SiC-AlN Diffusion Couple	9
IV.	Deposition of GaN PN Junctions and TEM Study of the Structure of AlN and GaN Films Deposited by a Modified Gas Source Molecular Beam Epitaxy System	18
V.	Distribution List	30

I. Introduction

The advent of techniques for growing semiconductor multilayer structures with layer thicknesses approaching atomic dimensions has provided new systems for both basic physics studies and device applications. Most of the research involving these structures has been restricted to materials with lattice constants that are equal within $\simeq 0.1\%$. However it is now recognized that interesting and useful pseudomorphic structures can also be grown from a much larger set of materials that have lattice-constant mismatches in the percent range. Moreover, advances in computer hardware and software as well as the development of theoretical structural and molecular models applicable for strained layer nucleation, growth and property prediction have occurred to the extent that the field is poised to expand rapidly. It is within this context that the research described in this report is being conducted. The materials systems of concern include combinations of the direct bandgap materials of AlN and GaN and selected, indirect bandgap SiC polytypes.

The extremes in thermal, mechanical, chemical and electronic properties of SiC allow the types and numbers of current and conceivable applications of this material to be substantial. However, a principal driving force for the current resurgence of interest in this material, as well as AlN and GaN, is their potential as hosts for high power, high temperature microelectronic and optoelectronic devices for use in extreme environments. The availability of thin film heterostructural combinations of these materials will substantially broaden the applications potential for these materials. The pseudomorphic structures produced from these materials will be unique because of their chemistry, their wide bandgaps, the availability of indirect/direct bandgap combinations, their occurrence in cubic and hexagonal forms and the ability to tailor the lattice parameters and therefore the amount of strain and the physical properties via solid solutions composed of the three components.

The research described in the following sections is concerned with the pseudomorphic nature and microstructural character of AlN/SiC and AlN/GaN layered assemblies. These sections detail the procedures, results, discussions of these results, conclusions and plans for future research. Each subsection is self-contained with its own figures, tables, and references.

II. Solid Solutions and Pseudomorphic Multilayer Heterostructures in the System AlN-SiC Produced by Plasma-assisted, Gas-source Molecular Beam Epitaxy

A. Introduction

Interest in wide band gap semiconductors for electronic and optoelectronic applications has increased greatly within the past several years. Two wide band gap materials which have generated much interest are SiC and AlN. SiC, the only binary compound in the Si-C system, is a prime candidate for high-power, high-temperature, and high-frequency electronic applications. It can form in many different polytypes; the most common of these are the cubic polytype, β- or 3C-SiC, and one of the hexagonal polytypes, 6H-SiC. However, since the band gap (3.0 eV for 6H-SiC, and 2.3 eV for β-SiC) is indirect, SiC cannot be used alone for optoelectronic applications. AlN is of particular interest for ultraviolet optical devices due to its large, direct band gap (E_g=6.28 eV). Typically, it forms in the wurtzite structure, although recent research showing cubic GaN grown on β-SiC [1] or GaAs [2] suggests it may be possible to form cubic AlN. In addition, cubic AlN has been grown on β-SiC in layers less than 100Å thick here at NCSU [3].

Solid solutions of AlN and SiC have been achieved by two primary routes: reactive sintering of mixtures of powders of a variety of sources and thin film deposition from the vapor phase. Matignon [4] first reported the synthesis of a $(AlN)_x(SiC)_{1-x}$ material in 1924 formed by heating Al_2O_3, SiO_2, and coke in the presence of flowing N_2 at an unspecified temperature. Related hot pressing and annealing research coupled with X-ray diffraction and optical and electron microscopy by Rafaniello *et al.* [5,6] reportedly resulted in single phase, 2H material at all compositions hot pressed at 2300°C but only within the ranges of 0–15 and 75–100 wt% AlN for samples prepared at 2100°C and below. This latter result indicated a miscibility gap, the existence of which was subsequently confirmed by Ruh and Zangvil [7], Zangvil and Ruh [8–10], Kuo and Virkar [11], and Czeka *et al.* [12] using a variety of heat treatment schedules. The tentative phase diagram proposed by Zangvil and Ruh [9] shows a flat miscibility gap at 1900°C between ≈ 20 and 80 wt% AlN. Above this temperature a 2H solid solution was reported from ≈ 20–100 wt% AlN. From 0–20 wt% AlN, solutions and two phase mixtures of 6H, 4H, and 2H were observed.

Thin film solid solutions have been produced in the Soviet Union [13] via sublimation of a sintered SiC/AlN compact at ≥ 2100°C and in the United States [14] using low pressure (10–76 Torr) metalorganic chemical vapor deposition (MOCVD) and the sources of SiH_4, C_3H_8, NH_3, and $Al(CH_3)_3$ carried in H_2. The former research also showed that at T ≥ 2100°C, solid solutions having the 2H structure could be produced at compositions of AlN ≥ 20 wt%. By contrast, Jenkins *et al.* [14], have reported the MOCVD growth of solid

solutions over the entire pseudobinary phase diagram. The composition of these films, grown from 1200–1250°C, was strongly dependent on the system pressure, which varied from 10–76 Torr. Electron channeling patterns on selected films indicated that the films were monocrystalline. Films having cubic symmetry were obtained on Si(100) substrates; hexagonal films were deposited on α(6H)-SiC (0001) wafers.

Epitaxial wurtzitic AlN has been deposited previously on SiC substrates [15–17]. Chu *et al.* [15] obtained monocrystalline AlN layers of up to 25 μm thickness on hexagonal SiC{0001} substrates by chemical vapor deposition (CVD) from 1200–1250°C. Sitar *et al.* [16] used an electron cyclotron resonance (ECR) plasma for decomposition of N_2 and Al and Ga effusion cells for growth of AlN/GaN superlattices by plasma-assisted, gas source MBE on α(6H)-SiC(0001) and Al_2O_3(0001) at 600°C. The thickness range of the AlN layers was 0.5–20nm. However, the properties of the individual AlN layers were not examined. Yoshida *et al.* [17] also employed gas–source MBE and the sources of solid Al and NH_3 to deposit single crystal AlN films on Si(111) and Al_2O_3(0001) and (01$\bar{1}$2) at 1000–1200°C. They noted their films were much smoother than CVD-grown material and rivaled bulk single crystal AlN. Conversely, Rutz and Cuomo [18] reported the deposition of monocrystalline SiC on a single crystal AlN film by pyrolysis of a SiC target at 1860°C. The AlN substrate was previously formed at 1000°C by reactive rf sputtering on a W(111) single crystal. However, thin-film growth of AlN/SiC/AlN or SiC/AlN/SiC heterostructures has not been reported to date.

Stable pseudomorphic heterostructures of AlN and SiC are feasible because of their similarity in crystal structure, lattice parameter and thermal expansion behavior. Theory regarding the electronic structure and bonding at SiC/AlN interfaces has been developed [19]. Critical layer thicknesses prior to misfit dislocation formation at pseudomorphic interfaces of cubic AlN and cubic SiC have been calculated [20]. Superlattices of these materials would have a different band structure than either constituent element because the Brillouin zone is reduced in size in the direction normal to the interfaces, and certain superlattice states occur at different points in k space than the corresponding bulk material [21]. This may allow the resultant superlattice to have a direct band transition.

B. Experimental procedure

All samples were grown on the Si and C faces of 6H-SiC(0001) substrates supplied by Cree Research, Inc. These vicinal 6H-SiC(0001) wafers oriented 3-4° towards [11$\bar{2}$0] contained a 0.8 μm epitaxial 6H-SiC layer deposited via CVD and a thermally oxidized 50 nm layer to aid in wafer cleaning. Substrates were chemically cleaned prior to growth in a 10% HF solution for five minutes to remove the oxide, immediately loaded into the growth system and heated for five minutes at the growth temperature of 1050 °C.

All growth experiments were carried out in the plasma-assisted, gas-source molecular beam epitaxy system detailed in previous reports. The sources of Si and C were Si_2H_6 and C_2H_4 (both 99.99% pure), respectively. Sources of Al and N were solid Al (99.999% pure) evaporated from a standard MBE effusion cell and electron cyclotron resonance decomposed N_2 (99.9995% pure), respectively. Typical base pressures of 10^{-9} Torr were used. Specific growth conditions for a particular solid solution composition (30% AlN) and a particular multilayer are shown in Tables I and II.

Table I. Conditions for $(AlN)_{0.3}(SiC)_{0.7}$ growth

Chamber Base Pressure	10^{-9} Torr
Deposition Pressure	10^{-4} Torr
Deposition Temperature	1050°C
Flow Rate (Si_2H_6)	0.75 sccm
Flow Rate (C_2H_4)	3.75 sccm
Ar:N_2 Ratio	20:1
ECR Microwave Power	100 W
Aluminum Cell Temperature	1260°C
Deposition Time	2 hours

Table II. Conditions for AlN/SiC multilayer growth

AlN		**SiC**	
Growth temperature	1050°C	Growth temperature	1050°C
Nitrogen flow rate	8 sccm	Disilane flow rate	2.0 sccm
Microwave power	100 W	Ethylene flow rate	0.50 sccm
Al Cell Temperature	1170°C	Chamber Base Pressure	10^{-9} Torr
Chamber Base Pressure	10^{-9} Torr	Deposition Time	30 min
Deposition Time	20 min		

Reflection high-energy electron diffraction (RHEED) at 10 kV and high-resolution transmission electron microscopy (HRTEM) were used for structure and microstructure

analyses. Samples were prepared for HRTEM using standard techniques [22]. An Akashi EM 002B high-resolution transmission electron microscope was used at 200 kV for the HRTEM analysis.

C. Results and Discussion

Figure 1 shows a HRTEM photograph of an $(AlN)_x(SiC)_{1-x}$ solid solution grown under the previously listed conditions. The smooth surface and the step features at this surface imply a two-dimensional, or layer-by-layer, growth mode. The random distribution of contrast, which is due to the elastic and plastic strains in the film, indicates the presence of lattice bending, dislocations along the basal (0001) plane, point defects such as vacancies and interstitials, and a possible mixture of phases. The ABABAB... stacking sequence is indicative of the wurtzite (2H) crystal structure. The selected area optical diffraction pattern shown in the inset is indicative of the $[11\bar{2}0]$ azimuth for the wurtzite crystal structure. The Auger depth profile shown in Figure 2 indicates the composition to be approximately $(AlN)_{0.3}(SiC)_{0.7}$.

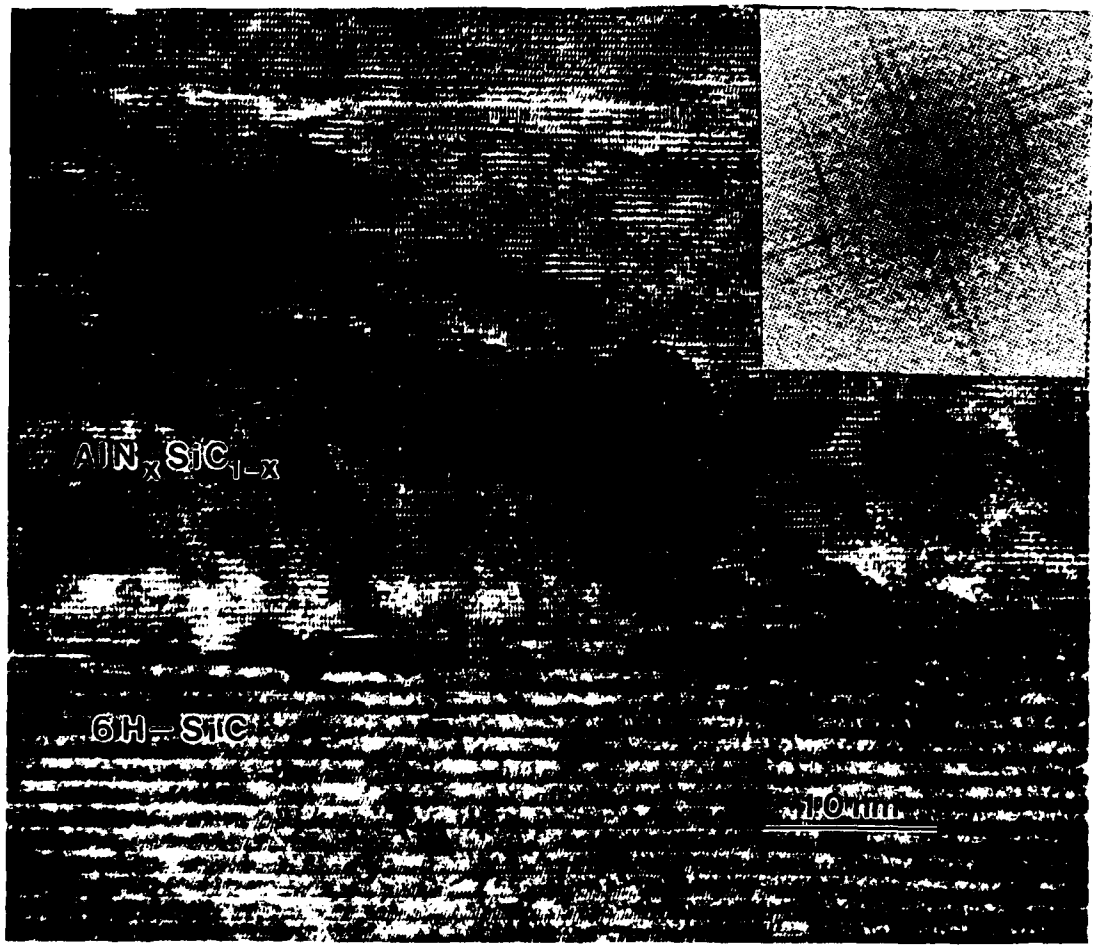

Figure 1. HRTEM image of $(AlN)_x(SiC)_{1-x}$ solid solution film on α(6H)-SiC(0001).

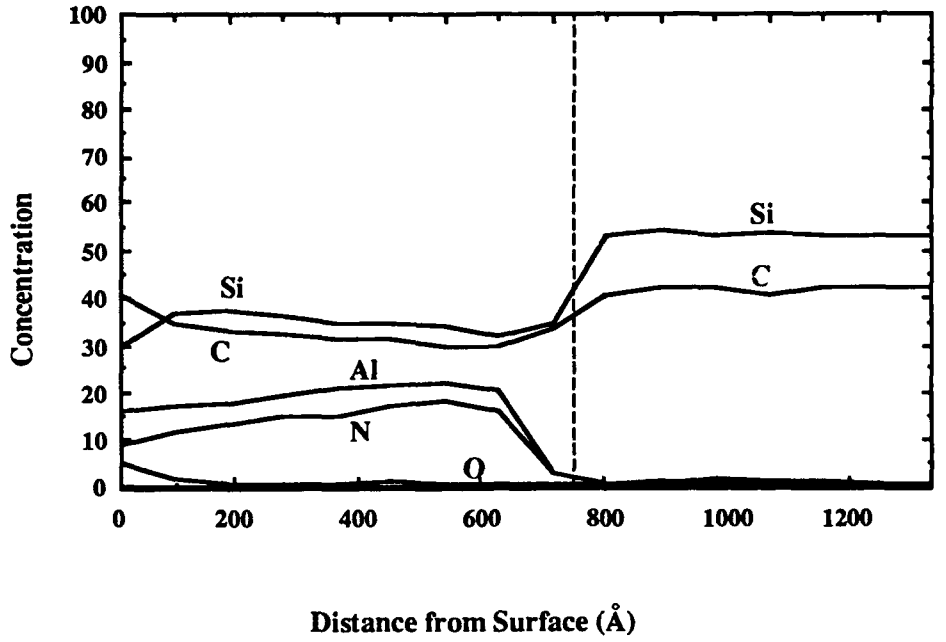

Figure 2. Auger depth profile of film shown in Figure 1.

Figure 3 shows an Auger depth profile of the multilayer produced using the conditions listed in Table II. This film consists of the α(6H)-SiC(0001) substrate, 2H-AlN, 3C-SiC, 2H-AlN and 3C-SiC. Each layer was shown to be monocrystalline by RHEED analysis as shown in Figs. 4 (a), (b), (c) and (d). These photographs were taken at the completion of each layer grown. At the present, no HRTEM analysis is available on these thin layers.

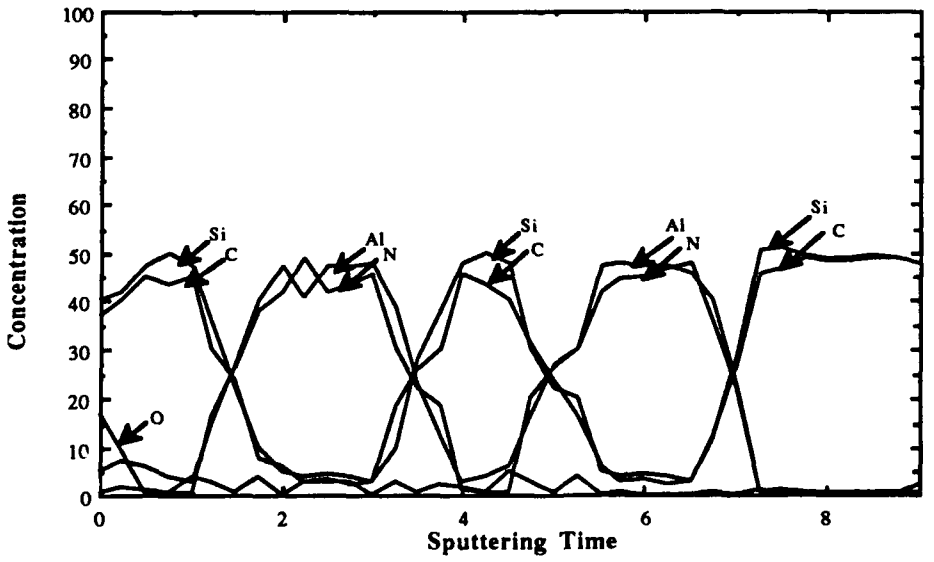

Figure 3. Auger depth profile of pseudomorphic heterostructure grown under conditions listed in Table II.

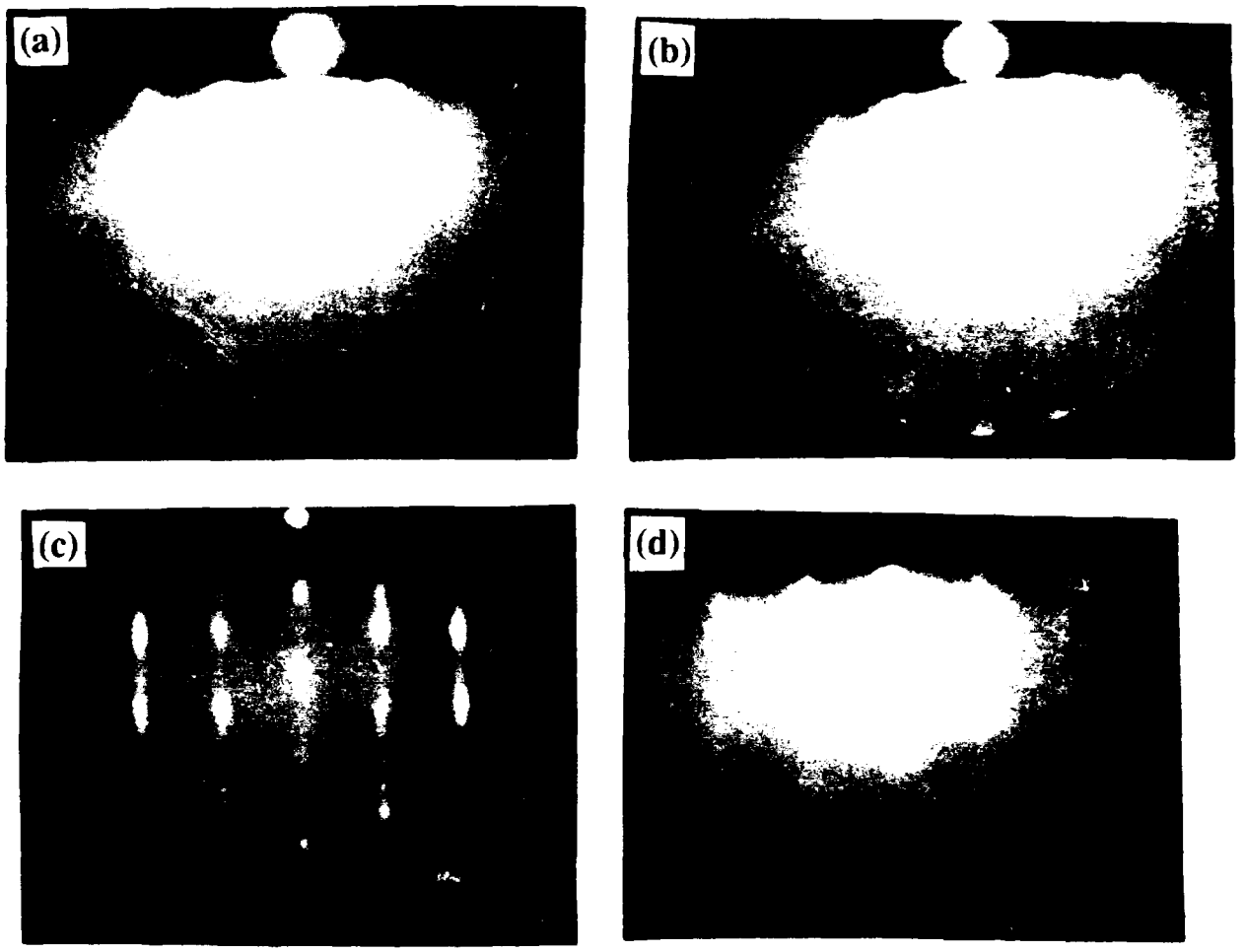

Figure 4. RHEED images of: (a) 2H-AlN, (b) 3C-SiC, (c) 2H-AlN and (d) 3C-SiC.

D. Conclusions

Solid solutions and pseudomorphic heterostructures of AlN and SiC have been grown on vicinal α(6H)-SiC(0001) substrates. RHEED, HRTEM and Auger depth profiling indicate the films to be monocrystalline. The solid solutions have the approximate composition $(AlN)_{0.3}(SiC)_{0.7}$ and have the wurtzite structure. The multilayers have the following components: α(6H)-SiC(0001) substrate, 2H-AlN and 3C-SiC.

E. Future Research Plans and Goals

A new heating element, manufactured by Advanced Ceramics, Inc., made of a composite graphite/boron nitride has been installed to replace the previously used tungsten filament. The new element has a rated T_{max} = 2500 °C and should allow for the expansion of the operating temperature range which is currently limited to a maximum of 1250 °C. Also, a new gas delivery system for mixtures of Ar and N_2 has been installed to allow for more precise control

of N flux arriving at the substrate, thus aiding in solid solution formation and control. Additionally, a RHEED oscillation and in situ monitoring system has been purchased and is presently being used to monitor the pre-deposition and initial deposition effects of temperature, cleaning procedure and reactant introduction on film quality.

F. References

1. M. J. Paisley, Z. Sitar, J. B. Posthill, and R. F. Davis, J. Vac. Sci. Technol. **A 7**, 701 (1989).
2. M. Mizuta, S. Fujieda, Y. Matsunomo, and T. Kawamura, Jpn. J. Appl. Phys **25**, L945 (1986).
3. Z. Sitar, Ph.D. Dissertation, North Carolina State University, Raleigh, NC, 1990.
4. C. Matignon, Compt. Rend. hu. L'Acad. Sci. **178**, 1615 (1924).
5. W. Rafaniello, K. Cho, and A. V. Vikar, J. Mat. Sc. **16**, 3479 (1981).
6. W. Rafaniello, M. R. Plinchta, and A. V. Vikar, J. Am. Ceram. Soc. **66**, 272 (1983).
7. R. Ruh and A. Zangvil, J. Am. Ceram. Soc. **65**, 260 (1982).
8. A. Zangvil and R. Ruh, Mat. Sc. Eng. **71**, 159 (1985).
9. A. Zangvil and R. Ruh, J. Am. Ceram. Soc. **71**, 884 (1988).
10. A. Zangvil and R. Ruh in *Silicon Carbide '87*, American Ceramic Society, Westerville, OH, 1989, pp. 63-82.
11. S. Kuo and A. V. Vikar, J. Am. Ceram. Soc. **73**, 2460 (1990).
12. C. L. Czkaj, M. L. J. Hackney, W. J. Hurley, Jr., L. V. Interrante, G. A. Sigel, P. J. Schields, and G. A. Slack, J. Am. Ceram. Soc. **73**, 352 (1990).
13. Sh. A. Nurmagomedov, A. N. Pitkin, V. N. Razbegaev, G. K. Safaraliev, Yu. M. Tairov, and V. F. Tsvetkov, Sov. Phys. Semicond. **23**, 100 (1989).
14. I. Jenkins, K. G. Irvine, M. G. Spencer, V. Dmitriev, and N. Chen, in press.
15. T. L. Chu, D. W. Ing, and A. J. Norieka, Solid-State Electron. **10**, 1023 (1967).
16. Z. Sitar, M. J. Paisley, B. Yan, R. F. Davis, J. Ruan, and J. W. Choyke, Thin Solid Films **200**, 311 (1991).
17. S. Yoshida, S. Mizawa, Y. Fujii, S. Takada, H. Hayakawa, S. Gonda, and A. Itoh, J. Vac. Sci. Technol. **16**, 990 (1979).
18. R. F. Rutz and J. J. Cuomo, in *Silicon Carbide-1973*, (U. of South Carolina Press, Columbia, 1974), p. 72.
19. W. R. L. Lambrecht and B. Segall, Phys. Rev. B **43**, 7070 (1991).
20. M. E. Sherwin and T. J. Drummond, J. Appl. Phys. **69**, 8423 (1991).
21. G. C. Osbourn, J. Vac. Sci. Technol. B **1**, 379 (1983).
22. J. C. Bravman and R. Sinclair, J. Electron Microsc. Tech. **1**, 53 (1987).

III. Determination of the Diffusivity of Si, C, Al and N at the Interface of the SiC-AlN Diffusion Couple

A. Introduction

Silicon carbide has long been of interest because of its superior structural, thermal and electrical properties. High temperature and/or erosion- and corrosion-resistant wear parts, as well as, optoelectronic and microelectronic semiconductor devices are representative applications. Control of the physical and chemical properties of SiC via microstructural changes achieved by using different processing routes has been extensively studied for many years. The microstructural variables most frequently changed include the amount and the morphology of the various polytypes in the processed material, intentionally introduced second and additional phases and additions of sintering aids which may or may not form a grain boundary phase. The processing temperature, impurity content, and sintering (or annealing) atmosphere affect the resultant microstructure. However, the primary material remains SiC. Another approach to property engineering involves the alloying of SiC with other ceramic compounds to alter, e. g., the band gap. This approach has also been of interest for several years.

One compound which has been reportedly alloyed with α(6H)-SiC (a_O = 3.08Å) is AlN (a_O = 3.11Å) due to the similarities in the atomic and covalent radii and the crystal structures. Diverse processing routes have been employed to achieve partial or complete solid solutions from these two compounds including reactive sintering or hot pressing of powder mixtures and thin film deposition from the vapor phase [2–5,8,16–20,22,23]. There exists, however, a difference in opinion among investigators regarding the occurrence and the extent of solid solutions in the SiC-AlN system at temperatures < 2100°C.

Schneider [1] concluded that the formation of $(AlN)_x(SiC)_{1-x}$ solid solutions of were not favorable within the temperature range of his study of the AlN-Al_4C_3-SiC-Si_3N_4 system. He found two phase mixtures rather than $(AlN)_x(SiC)_{1-x}$ solid solutions when equal molar ratios of either SiC and AlN or Si_3N_4 and Al_4C_3 were hot pressed at 1760°C–1860°C for 45 and 30 minutes, respectively. Subsequently, Zangvil and Ruh [4] prepared sintered samples of varying compositions by cold pressing powdered mixtures of SiC and 10–50 wt % AlN and subsequently hot-pressing them in vacuum. Microstructures of the samples hot-pressed within the range 1850–1950°C revealed partially sintered AlN grains and β-SiC grains of unusually large size. Ruh [2,19,26] using dry mixtures of SiC and AlN powders, hot-pressed in vacuum under the conditions of 35MPa and 1700–2300°C obtained no SiC-AlN solid solution for temperatures ≤ 2100°C and concentrations of ≈35 to 100 mol % AlN. In contrast, Rafaniello [8] reported solid solutions as indicated by X-ray diffraction in samples only hot-pressed at 1950°C–2300°C and 70 MPa for ≈3 h in Ar. However, he subsequently showed [3] using a

more careful analysis of his X-ray diffraction data that the broadening of the SiC-AlN peak was caused by the existence of a two-phase region and not the 2H solid solution previously reported [8]. The initial confusion was caused by the closeness (≈1%) in the lattice parameters of SiC and AlN. This was supported by optical microscopy of multiphase assemblages in the sintered samples for temperatures as high as 2300°C. Rafaniello [3] also revealed strong evidence of a miscibility gap by the precipitation of SiC-rich phase from 75 wt % AlN solid solution and precipitation of an AlN-rich phase from a 47 wt % AlN alloy, when hot-pressed samples were annealed at 1700°C for 90h. Modulated structures were found by Kuo [5] for samples with equimolar compositions below ≈ 1900°C and in samples containing 25 mol % SiC - 5 mol % AlN annealed at 1700°C for 170 h. Likewise, Chen [22] hot-pressed a mixture of β-SiC and AlN powders in nitrogen at ≈2300°C for 20 min to 3.5 h. Samples were then annealed in nitrogen (1 atm) over a range of temperatures between 1600°C–2000°C for up to 1145 h. Modulated structure development in samples of equimolar composition annealed at 2000°C and below indicated that 2000°C is below the coherent spinodal which would give further evidence of a miscibility gap as reported by Rafaniello [3], Kuo [5] and Sugahara [6].

Common to all the investigations described above was the use of AlN and β-SiC powders supplied by Herman Starck and the high concentrations of impurities contained in these materials. The concentration of oxygen and boron in starting powders [2–5,8,18–20,22,23] is significant. Xu and Zangvil [18] found small Al_2O_3 inclusions embedded in 2H grains of SiC-AlN samples uniaxially prepressed at room temperature to 35 MPa and subsequently hot-pressed at 2150°C at a pressure of 40 MPa in a flowing nitrogen atmosphere (1 atm.). The oxygen needed for the formation of the Al_2O_3 inclusions was beyond the 2% content reported in the analysis of the as-received AlN and, therefore, was probably introduced during processing. This is of considerable importance since Tajima [9] found that in the temperature range of 1800°C–2000°C the solid solubility of aluminum in SiC may be influenced by impurities and by the heating atmosphere; since, the defect structure of SiC would be affected by these factors. He also found conclusive evidence that aluminum atoms substitute for silicon in SiC. Furthermore, Zangvil [4] suggested that aluminum and nitrogen move as well as silicon and carbon as diffusion couples to ensure a local charge balance during mass transport. This process would be strongly impurity dependent and therefore control the solid solution formation. Oden [20] attempted to deal with the issue of impurities by preparing Al_4C_3 and SiC and comparing these with Hermann Starck- SiC and Cerac- AlN. The impurities of the latter materials were reported, however, those contained in Oden's materials were not. It was suggested by Oscroftt [21] that the oxygen content present in both materials was very high. Furthermore, the highly reducing nature of the graphite hot-pressing die may be the controlling factor in the oxygen content for both pure and impure materials [21]. Further evidence of the effects of oxygen was presented in a later study by Kuo [27] who found the existence of an

extensive, if incomplete, solid solution between AlN and Al_2OC at temperatures in excess of 1900°C. Below about 1800°C, the 2H solid solution was unstable and decomposed into two solid solutions of 2H crystal type as shown by the presence of extremely fine precipitates developed during cooling. The kinetics of solid solution formation were relatively rapid when compared with the SiC-AlN system, assuming such solutions actually occur in this latter system. This is of considerable importance when considering the high oxygen content in starting AlN materials. It should also be noted that two different phase diagrams have been presented for the SiC–AlN system Zangvil and Ruh [26] and Patience [30]. The most widely accepted was proposed by Zangvil and Ruh [26]. It is based on data obtained from numerous sintering experiments [2-4,8,19].

In contrast to the studies described above are reports of the formation of solid solutions between SiC and AlN at relatively low processing temperatures (i.e. within the proposed miscibility gap region). Cutler [7] formed solid solutions between SiC and AlN from 2 mol % to 100 mol % AlN with a single wurtzite type phase, as determined by X-ray diffraction. This was accomplished by the carbothermal reduction of fine amorphous silica ('cabosil'), precipitated aluminum hydroxide, and a carbon source of starch/sugar in a nitrogen atmosphere at 1400°C–1600°C. In subsequent work, by Rafaniello [8], intimate mixtures of SiO_2, Al_2O_3 and C were reacted at 1650°C for 4 h in flowing N_2. Solid solutions over the entire composition range were reported.

Processing conditions and impurities were shown to be a factors affecting the solid solution formation by Czekj [24]. He prepared solid solutions of 2H-$(AlN)_x(SiC)_{1-x}$ from rapid pyrolysis ("hot drop") of organometallics at temperatures < 1600°C. In contrast, slow pyrolysis of mixtures produced compositions rich in 2H-AlN and 3C-SiC at 1600°C which were later transformed to 2H-$(AlN)_x(SiC)_{1-x}$ solid solutions after heating to 2000°C. Jenkins, *et al.* [16] reported the growth of solid solutions of $(AlN)_x(SiC)_{1-x}$ by MOCVD over the entire composition range from 20 % to 90 % AlN in the temperature range of 1200°C–1250°C, as measured by Auger spectroscopy. Kern [17] reported growth of a high purity $(AlN)_{0.3}(SiC)_{0.7}$ solid solution at 1050°C by plasma-assisted gas source molecular beam epitaxy.

Theoretical calculations of the immiscibility region in the $(AlN)_x(SiC)_{1-x}$ system were conducted by Sukhanek [28] using the dielectric theory of A^NB^{8-N} semiconductors. The theory relates changes in the band structure to the enthalpy of formation in semiconductors. He concluded that the formation of a continuous series of solid solutions of silicon carbide with aluminum nitride were possible above 1000°K. This was shown by Shimada [10] who hot pressed mixtures of SiC, Si_3N_4, AlN and Al_3C_4 powders at 1300°C - 1900°C and 3.0 GPa for 1 h and reported the formation of solid solutions by X-ray diffraction. Tsukuma [11] also sintered mixtures of Si_3N_4 and Al_4C_3 in a gas autoclave at 1800°C and 10 MPa in argon. Solid solutions rich in AlN were produced. However, solutions in the SiC-rich region could not be

formed under the same conditions. Zangvil [12] suggested that this phase was a solid solution of $(AlN)_x(SiC)_{1-x}$ based on lattice parameters; however he also noted that he found no solid solution at 1900°C in vacuum and that Schneider [1] did not form solid solutions at 1860°C. It is interesting to note the short processing time < 1 h. Tsukuma's [11] findings are consistent with the proposed kinetics and reaction path described by Rafaevich [29] and Mitomo [15].

Rafaevich [29] used conditions similar to Zangvil [4] to determine the kinetics of the reaction between Si_3N_4 and Al_3C_4. The purpose of his work was to determine the formation mechanism of the $(AlN)_x(SiC)_{1-x}$ solid solutions during sintering. Diffraction patterns after sintering for 0.5 h at 1950°C in 1 atm of nitrogen indicated that SiC had not completely formed and that Si_3N_4 was still present. Sintering for 1 h at 1950°C indicated that Si_3N_4 had completely transformed into SiC; however, solid solutions of SiC-AlN had not completely formed. Sintering for 1.5 h at 1950°C showed a complete, homogeneous $(AlN)_x(SiC)_{1-x}$ solid solution. Reaction paths studied by Mitomo [15] were determined by the formation of a uniformly dispersed composite powder of β-SiC and 2H-AlN using an alkoxide-derived SiO_2-Al_2O_3 mixture. The total reaction was carried out at 1500°C and of the form:

$$2SiO_2 + Al_2O_3 + 9C + N_2 \rightarrow 2SiC + 2AlN + 7CO$$

The large amounts of carbon (3.7 time the normal amount) were needed to complete the reaction. Reactions observed at 1500°C were

$$2SiO_2 + Al_2O_3 + 10.5C \rightarrow 1.5SiC + 0.5Al_4SiC_4 + 7CO$$

$$1.5SiC + 0.5Al_4SiC_4 + N_2 \leftrightarrow 2SiC + 2AlN + 1.5C$$

Large weight loss after the reaction was attributed to the evaporation of SiO_2 as SiO. Mitomo [15] suggested that SiO_2 and Al_2O_3 reacted in sequence with carbon. This is of substantial use in the evaluation of the reported attempts to form solid solutions which have been previously published. The indication is that the formation of $(AlN)_x(SiC)_{1-x}$ solid solutions using SiO_2 and Al_2O_3 in a N_2 atmosphere is not favorable for short sintering times due to the complex reaction scheme.

Zangvil [4] has approximated the diffusion coefficients between SiC and AlN to be 10^{-12} $cm^2 \cdot s^{-1}$. The corresponding activation energy and pre-exponential term were estimated to be as high as 900 kJ·mol, and 10^{-8} $cm^2 \cdot s^{-1}$, respectively. Three reasons for these values were suggested by Zangvil [4]: (1) SiC penetration among AlN grains in the early stages of sintering (2) material transport by gaseous species, and (3) lattice diffusion of coupled SiC and AlN pairs.

The purpose of this investigation has been to determine the extent of solid solution formation within the temperature range of 1700°C–1850°C and to determine the diffusion

coefficients and the corresponding activation energies for the four elements Si, C, Al and N within this solution. It is clear that the atomic behavior and the extent of phase formation at relatively low temperatures for thin film deposition cannot be discerned from the research conducted previously. Likewise, the diffusivities of these species have not been studied for epitaxially deposited AlN on single crystal SiC.

B. Experimental Procedures

Sample Preparation. Samples were prepared in a modified Perkin-Elmer 430 molecular beam epitaxy (MBE) system. Aluminum (99.999%) was evaporated from a standard effusion cell. Activated nitrogen was achieved using an MBE compatible, electron cyclotron resonance plasma source. Single crystal AlN with very few planar defects was epitaxially deposited on vicinal α(6H)-SiC [0001] wafers manufactured by Cree Research, Inc. and cut off axis 3°–4° toward [11$\bar{2}$0]. Growth conditions for the films are presented in Table I.

Table I. Growth Conditions for the 2H AlN films on α(6H)-SiC(0001) substrates

Nitrogen pressure	2×10^{-4} Torr
Nitrogen flow rate	4–5 sccm
ECR microwave power	50 W
Substrate temperature	650°C
Growth rate	≈ 0.1μm/hr
Total growth time	7–8 hrs.

Transmission electron microscopy (TEM) (Hitachi H-800) photos have been taken of the 2H-AlN (wurtzite) film on the α(6H)-SiC substrate before annealing and show a smooth and abrupt interface. Several different precautions were taken in order to prevent contamination of the samples and to minimize the loss of volatile components principally aluminum, and nitrogen. The samples were placed in a high density pyrolitic graphite crucible shown schematically in Fig. 1. The inside of the crucible was previously coated with SiC by heating a mixture of Si and β-SiC inside the holder to 2000°C. The diffusion samples were placed inside this holder with the α(6H)-SiC(0001) face against the SiC coating. Bulk AlN squares were then placed on top of the deposited AlN. The holder was then closed using a threaded lid and loaded into the furnace. The chamber was evacuated (2×10^{-6} torr) to prevent contamination during diffusion. N_2 gas (99.9995%), purified by a gettering furnace containing heated Cu chips (Centorr Furnace model 2B-2O) was then introduced into the chamber at a rate of

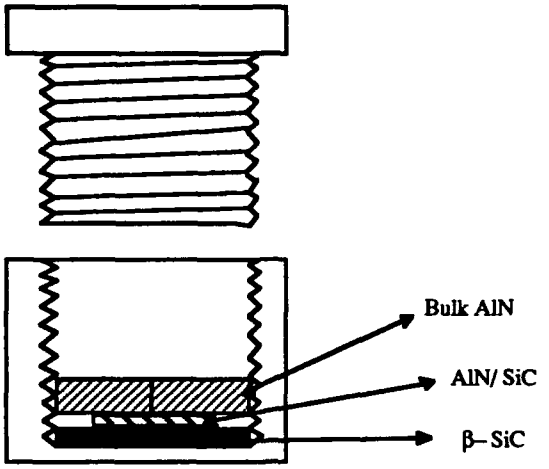

Figure 1. Schematic of a high density pyrolitic graphite crucible.

365 sccm. The chamber was brought to atmospheric pressure and a flowing N_2 environment maintained throughout each diffusion anneal. Diffusion temperatures were reached in ≈20 min (exact value for 1850° C). The samples were then removed for characterization. The N_2 gas, bulk AlN, and SiC coated crucible are not meant to aid in the diffusion. This was checked by a SiC-AlN standard which had not been annealed. The AlN as well as the SiC intensity in the standard were the same as AlN and SiC intensity outside of the diffused region. The samples were diffused for a temperature range of 1700°C to 1850°C for as wide a range of times as possible. A complete listing of temperatures and times are given in Table II.

Table II. Annealing conditions used to date for the AlN/SiC diffusion couples

Sample #	Temperature (°C)	Time (hrs)
32	1850	25
28	1850	21.5
21	1850	10
26	1800	30
31	1800	25
29	1800	20
27	1750	70
23	1750	50
18	1750	25
33	1700	70
19	1700	30

Characterization–Auger Spectroscopy. Scanning Auger microprobe (SAM) (JEOL JAMP-30) analysis was used to determine the concentration verses diffusion distance for all samples in Table II. Samples were tilted at a 60° angle in order to minimize charging effects. An argon ion sputtering unit attached to the SAM was used to sputter through the samples while data was being collected. Sputter rates were determined for the Ar ion beam in three different types of media namely, AlN, SiC and their solid solutions. This was accomplished by 5, 10 and 15 minute sputter rates on AlN and SiC then extrapolated for longer times in each medium. The depths were measured using a profilometer. The sputter rates for the solid solution region were determined by measuring the depth of different samples of different sputter times where the ion beam had sputtered through the entire diffused region and subtracting the sputter times for AlN and SiC. This rate was plotted and extrapolated for longer times. Knowing sputter rates for each material allowed for the conversion of sputter time to distance. Sputter rate standards also served as standards for the 100% intensity peaks for Al, N, Si, and C from which relative concentrations were obtained.

Characterization–Transmission Electron Microscopy. The samples was cut into 3 micron wide and 500 micron thick discs which were mechanically thinned to about 100 microns and dimpled at the SiC-AlN interface to a final thickness of 20 microns. Further thinning of the samples with an ion miller achieved an electron transparent area. An acceleration voltage of 6 kV for initial milling was used; it was decreased to 4 kV for the final milling. The milling angles of 15°, 12°, and 6° were used in sequence during the milling. TEM observations were subsequently conducted using Akashi EM-002B Ultra-High Resolution TEM at 200 kV. The TEM was conducted only on the longest runs to demonstrate microstructure.

C. Results

From Auger depth profiles it is apparent that diffusion has occurred and from the smoothness of the concentration verses distance profiles there is no indication of a two-phase region for samples annealed between 1700°C–1850°C. This indicates that complete solid solution formation over the entire composition range has been obtained. Using calculated sputter rates, values of concentration verses diffusion distance were determined. The Boltzmann-Matano diffusion equations were used to determine the diffusion coefficients for each element. It is possible that the α(6H)-SiC is transformed to the 2H-SiC polytype as a result of its initial contact with the AlN. If this is true, the calculated activation energy should be reduced by the amount of energy needed to transform the α(6H)-SiC to 2H-SiC. The solid solution subsequently occurs between the 2H-SiC and 2H-AlN via coupled diffusion in order to maintain local charge equilibrium. It should be noted that this is not the only means of forming the 2H solid solution. It is also possible that the diffusion of AlN into SiC causes the

transformation of SiC to the polytype 2H. In this case the reduction of the activation energy by the transformation energy may be incorrect.

In order to determine the diffusivities of the four components of the process the Boltzmann-Matano solution of the diffusivity, D, as a function of concentration, distance, and time (c, x, t) is being employed. At this writing, the Auger data is being carefully analyzed to ensure that diffusion has actually occurred between these two materials. The reason for this uncertainty is derived from the fact that in a parallel investigation of the apparent diffused region using electron energy loss (EELS) in cross-sectional TEM with a 15Å beam, the presence of Al and N as well as Si and C have not been observed in the SiC layer and the AlN film, respectively. Bright field TEM of the surface in cross section has revealed a stepped surface with very high steps. As such, it is important to make absolutely sure that the Auger electron beam is not detecting components from two different steps and thus giving an apparent diffusion profile rather than providing data of a real profile from the formation of solid solutions.

D. Future Research

Additional diffusion anneals will be conducted between 1750 and 2000°C using the same procedure described above. Special care will be used to ensure that a flat AlN surface is achieved after the diffusion experiments and prior to the Auger Depth profile studies. A quartz flat coupled with a He lamp will be used to check the flatness of the AlN surface. Light polishing with diamond paste will be used to produce the flat surface if it is not present after the diffusion anneals. Additional studies to be conducted in tandem with the diffusion runs include (1) the fabrication of solid solutions using MBE and the subsequent annealing at high temperatures to determine if either segregation of the AlN and SiC occurs or if the solid solution is maintained, thus proving that it is an equilibrium phase and (2) the additional use of EELS to determine if interdiffusion can be discerned at any temperature.

E. References

1. G. Schneider, L. J. Gauckler and G. Petzow, Material Science Monographs **6**, 399 (1980).
2. R. Ruh, A. Zangvil, J. Am. Ceram. Soc. **65** [5], 260 (1982).
3. W. Rafaniello, M. R. Plichta, A. V. Virkar, J. Am. Ceram. Soc. **66** [4], 272 (1983).
4. A. Zangvil, R. Ruh, J. Mat. Sci. and Eng. **71**, 159 (1985).
5. S. Kuo, A. V. Virkar, W. Rafaniello, J. Am. Ceram. Soc. **70** [6], C-125 (1987).
6. Y. Sugahara, K. Sugimoto, H. Takagi, K. Kuroda, C. Kato, J. Mat. Sci. Lett. **7**, 795 (1988).
7. I. B.Cutler, P. D. Miller, W. Rafaniello, H. K. Park, D. P. Thompson and K. H. Jack, Nature **275**, 434 (1978).
8. W. Rafaniello, K. Cho, A. V. Virkar, J. Mater. Sci. **16** [12], 3479 (1981).
9. Y. Tajima, W. D. Kingery, Am. Ceram. Soc. [2], C-27 (1982).

10. M. Shimada, K. Sasaki, M. Koizumi, Proc. of Inter. Sym. on Ceram. Components for Engines, (1983).
11. K. Tsukuma, M. Shimada, M. Koizumi, J. Mater. Sci. Lett. **1**, 9 (1982).
12. A. Zangvil, R. Ruh, J. Mater. Sci. Lett. **3**, 249 (1984).
13. K. A. Schwetz and A. Lipp, in *Am. Ceram. Soc.* 89th Annual meeting abstracts, The American Ceramic Society, Westerville, OH, p. 30, 1987.
14. R. A. Youngman, J. H. Harris, J. Am. Ceram. Soc., **73** [11], 3238-46 (1990).
15. M. Mitomo, M. Tsutsumi, Y. Kishi, J. Mat. Sci. Lett. **7**, 1151-1153 (1988) .
16. I. Jenkins, K. G. Irvine, M. G. Spencer, V. Dmitriev, N. Chen, J. Cry. Gro. **128** 375-378 (1993) .
17. R. S. Kern, L. B. Rowland, S. Tanaka, R. F. Davis, "Solid solutions of AlN and SiC grown by plasma-assisted, gas-source molecular beam epitaxy," J. Mat. Res.
18. Y. Xu, A. Zangvil, M. Landon, F. Thevenot, J. Am. Ceram. Soc. **75** [2], 325-333 (1992).
19. R. Ruh, A. Zangvil, J. Barlowe, Am. Ceram. Soc. Bull., **64** [10], 1368-1373 (1985).
20. L. L. Oden, R. A. McCune, J. Am. Ceram. Soc. **73** [6], 1529-1533 (1990).
21. R. J. Oscroft, D. P. Thompson, J. Am. Ceram. Soc. **74** [9], 2327-2328 (1991).
22. J. Chen, Q. Tian, A. V. Virkar, J. Am. Ceram. Soc. **75** [4], 809-821 (1992).
23. S. Y. Kuo, Z. C. Jou, A. V. Virkar, W. Rafaniello, J. Mat. Sci. **21**, 3019-3024 (1986).
24. C. L. Czekaj, M. Hackney, W. Hurley, L. Interrante, G. Sigel, P. Schields, G. Slack, J. Am. Ceram. Soc. **73** [2], 352-357 (1990).
25. A. Zangvil, R. Ruh, Silicon Carbide, 63-82 (1988).
26. A. Zangvil, R. Ruh, J. Am. Ceram. Soc. **71**[10], 884-890 (1988).
27. S. Kuo, A. V. Virkar, J. Am. Ceram. Soc. **72** [4], 540-550 (1989).
28. G. Sukhanek, Y. M. Tairov, V. F. Tsvetkov, Pis'ma Zh. Tekh. Fiz. **8** [12], 739-741 (1983).
29. N. B. Rafaevich, V. F. Tsvetkov, A. N. Komov, S. G. Losevskaya, Iz. Aka. Nauk SSSR, Neorg. Mater. **26** [5], 973-977, (1990).
30. M. M. Patience, P. J. England, D. P. Thompson , K. H. Jack, *Proc. of Inter. Sym. on Ceram. Components for Engine*, p. 473-479 (1983) Japan.

IV. Deposition of GaN PN Junctions and TEM Study of the Structure of AlN and GaN Films Deposited by a Modified Gas Source Molecular Beam Epitaxy System

A. Introduction

Most recently, the research of GaN PN junction type light emitting diodes (LED) has made significant progress. Several groups have reported that GaN PN junctions have been successfully deposited, and have observed blue light emission [1–4]. However, to date, all reported GaN PN junction LED devices were made by a MOCVD technique. In addition, to exhibit P-type character, Mg-, or Zn-doped GaN films still need post-growth treatment, such as post-deposition Low-Energy Electron-Beam Irradiation (LEEBI) or annealing at high temperatures in a nitrogen environment.

In the last report, we had shown that by a modified gas source molecular beam epitaxy system (GSMBE), we were able to deposit p-type Mg-doped GaN films directly, i.e., without any post-growth treatment. In this report, we will show the further success of the deposition of GaN PN junctions by GSMBE.

Also in this report, we will show microstructural analysis by transmission electron microscopy of our AlN and GaN films deposited under various different growth conditions.

B. Experimental Procedure

The deposition system employed in this research was a commercial Perkin-Elmer 430 MBE system. This system consists of three parts: a load lock (base pressure of $5*10^{-8}$ Torr), a transfer tube (base pressure of $1*10^{-10}$ Torr), which also was used for degassing the substrates, and the growth chamber (base pressure of $5*10^{-11}$ Torr). Knudson effusion cells with BN crucibles and Ta wire heaters were charged with 7N pure gallium, 6N pure aluminum, 6N pure magnesium and 6N pure silicon respectively. Ultra-high purity nitrogen, further purified by a chemical purifier, was used as the sources gas. The nitrogen gas was excited by an ECR plasma source, which was designed to fit inside the 2.25 inch diameter tube of the source flange cryoshroud. The details of the system can be found elsewhere [5].

The substrates were (0001) oriented α(6H)-SiC wafers obtained from Cree Research, Inc. Prior to loading into the chamber, the α-SiC substrates were cleaned by a standard degreasing and RCA cleaning procedure. All substrates were then mounted on a 3-inch molybdenum block and loaded into the system. After undergoing a degassing procedure (700°C for 30 minutes), the substrates were transferred into the deposition chamber. Finally RHEED was performed to examine the crystalline quality of the substrates.

C. Results

Deposition of GaN PN Junctions. Based on previous research results of the deposition of individual p-type Mg-doped GaN and n-type Si-doped GaN films, we have deposited the GaN PN junctions by a two-step and one-mask process.

We first deposit Si-doped GaN on the substrate. During this step, we initially expose the substrates to pure Al followed by exposure of this Al to the plasma activated nitrogen species in order to form an AlN layer. By this procedure, we have eliminated a thin amorphous layer on the substrate surface due to the plasma exposure. The film growth was subsequently started using the deposition conditions listed in Table I. An AlN buffer layer, having a thickness of about 150Å, was used to reduce the lattice mismatch and was followed by a layer of Si-doped GaN, which was ~3000Å thick.

Table I. Deposition Conditions for Si-doped GaN Films

Nitrogen pressure	2×10^{-4} Torr
Microwave power	50W
Gallium cell temperature	990°C
Aluminum cell temperature	1120°C
Silicon cell temperature	1180°C
substrate temperature	650°C
Al layer	2 monatomic layer
AlN buffer layer	150~200Å
Si-doped GaN	3000~4000Å

Then the sample was taken out of the system and a mask with defined open area was put on the top of the sample. With this mask we can make electrical contacts on the covered area of n-type Si-doped GaN, since we do not have a GaN etching facility to form the contacts.

Secondly, a layer of Mg-doped GaN (~3000Å thick) was deposited on the masked n-type GaN film by the conditions listed in Table II.

Characterization of GaN PN Junctions. Currently, we have only made IV measurements on these GaN PN junctions. The contacts for the measurement were made by two spring probes. IV curves were measured by a Hewlett Packard 4145 Semiconductor Parameter Analyzer. Typical IV curves are shown in Fig. 1 for the GaN PN junction on a sapphire substrate and in Fig. 2 for the GaN PN junction on an α-SiC substrate. The p-type character of the top Mg-doped GaN films was verified by the hot probe method.

Table II. Deposition Conditions for Mg-doped GaN Films

Nitrogen pressure	2*10-4 Torr
Microwave power	50W
Gallium cell temperature	990°C
Magnesium cell temperature	~300°C
substrate temperature	650°C
Mg-doped GaN	3000~4000Å

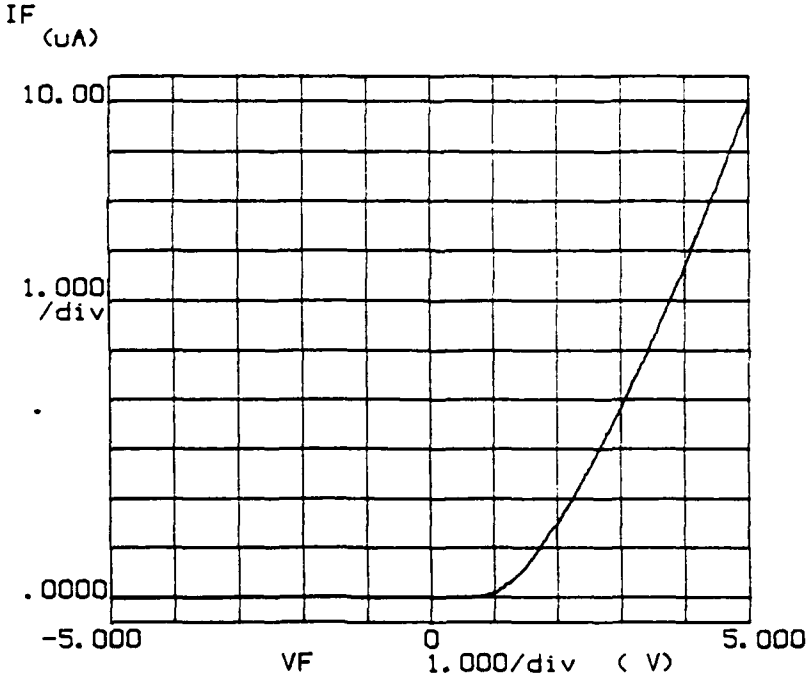

Figure 1. IV curve for the GaN PN junction on (0001) sapphire substrate.

Rectifying characteristics have been observed for the PN GaN junctions on both α-SiC and sapphire substrates. The turn-on voltages for both junctions are about 2 volts. At the same bias, the forward current for the junction on an α-SiC substrate is much larger than the junction on a sapphire substrate.

Further investigation of these junctions is underway, such as ohmic-metal contacts on either n- or p-type GaN layers, reactive ion etching of GaN films in order to deposit n- and p-type GaN layers without interruption, as well as electroluminescence measurements.

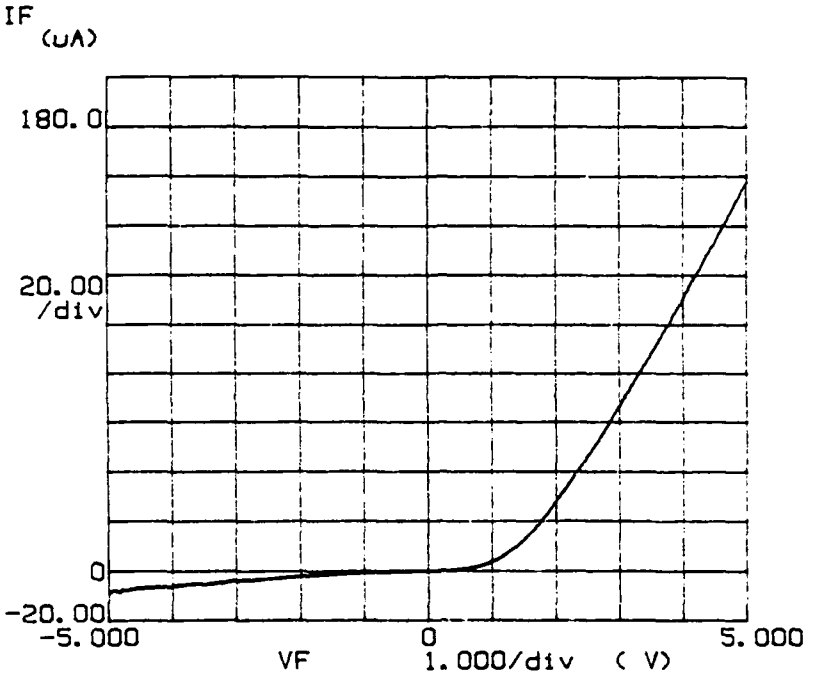

Figure 2. IV curve for the GaN PN junction on (0001) α-SiC substrate.

Electron Microscopy Characterization of AlN and GaN Films. The microstructure of the nitride films deposited by GSMBE was characterized by Transmission Electron Microscopy (TEM). The effect of various deposition conditions on the microstructure was investigated.

The TEM was performed in a JEOL 4000EX operated at 400kV. High resolution images were recorded using a 1mr convergence semi-angle at Scherzer defocus (~ -47nm). Cross-sectional transmission electron microscopy (XTEM) samples were prepared using standard techniques.

TEM Characterization of AlN Films. Previously, high quality AlN films had been deposited as buffer layers for the growth of GaN films using a modified GSMBE system. High resolution TEM indicated that these films had a highly oriented columnar structure [6]. Here we have investigated any structure change with respect to an increase in film thickness. As shown in Fig. 3, when the film thickness is increased above the critical thickness while maintaining the same deposition conditions, the density of defects which are parallel to the growth surface has greatly increased. The average width of the columnar features is about the same as that seen in the thin, ~100Å, AlN buffer layers. Both AlN films exhibited single crystal RHEED patterns.

The deposition temperature of our AlN films (~650°C) is much lower than what is most commonly used for MOCVD (above 1000°C). To improve the quality of the AlN films, the deposition temperature was raised to 1100°C while keeping other conditions the same. Figure 4

Figure 3. TEM micrograph of an AlN film deposited at 650°C.

is a TEM micrograph of an AlN film deposited at this higher temperature, 1100°C. Defects running perpendicular to the substrate have been greatly reduced, and defects parallel to the growth surface have been removed. A high resolution TEM micrograph of this AlN film, Fig. 5, shows the epitaxial AlN/α-SiC interface.

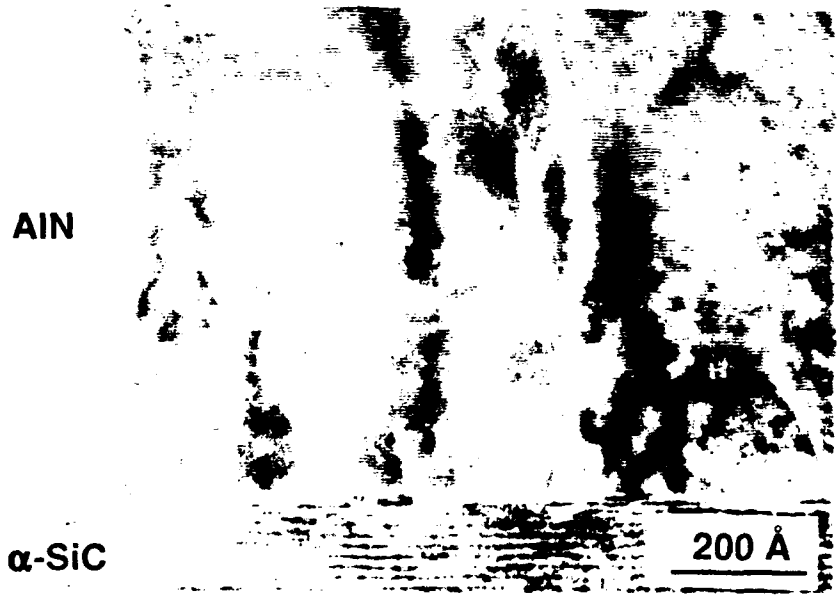

Figure 4. TEM micrograph of an AlN film deposited at 1100°C.

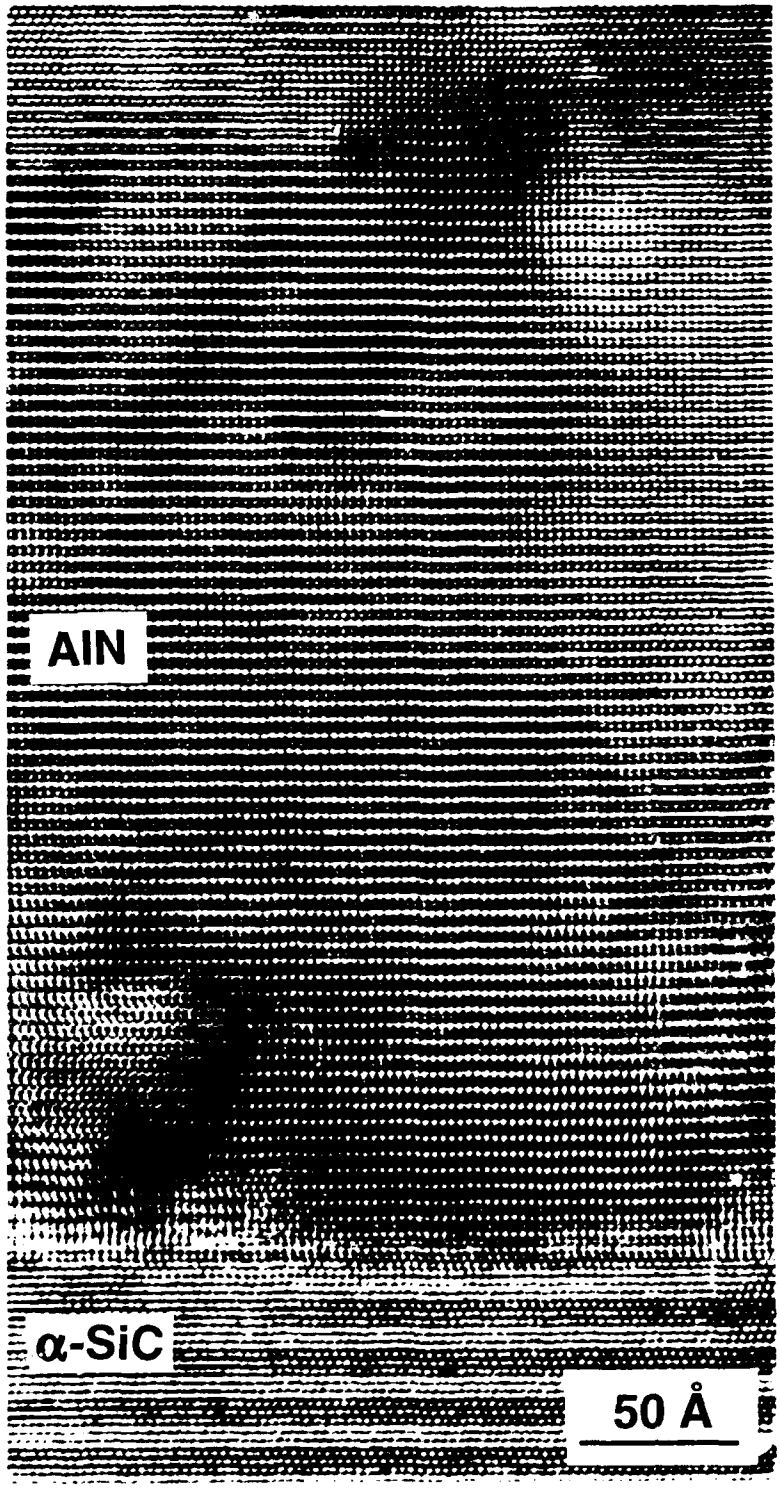

Figure 5. HRTEM micrograph of AlN film deposited at 1100°C.

TEM Studies of GaN Films. By a modified gas source molecular beam epitaxy system high quality GaN films have been deposited on both sapphire and α-SiC substrates [6]. RHEED, X-ray diffraction and electron diffraction have indicated that the films are single crystalline. However, as we reported before, TEM revealed that the GaN films still had a columnar

structure. In order to reduce or eliminate these columnar features, we have investigated the effects of various different growth conditions. We limited our study to GaN films deposited on (0001) α-SiC substrates.

The TEM micrographs shown in Fig. 6 are of two GaN films deposited under the same growth conditions except for differing buffer layers. The film shown in Fig. 6 (a) has an AlN buffer layer for which the AlN was deposited at the same temperature as the GaN (650°C), while in Fig. 6 (b), there is no buffer layer. In the film with the buffer layer, there are fewer defects in the GaN close to the AlN buffer layer although increase in number further from the buffer layer. Comparison of Figs. 6 (a) and (b) reveals that the film without the buffer layer has more defects which are parallel to the growth surface and more of a columnar structure than the film with the buffer layer (with respect to the region of GaN close to the buffer layer). Since we know that the growth of high quality, epitaxial AlN films has been achieved at a higher deposition temperature on α-SiC substrates, we have attempted to eliminate the

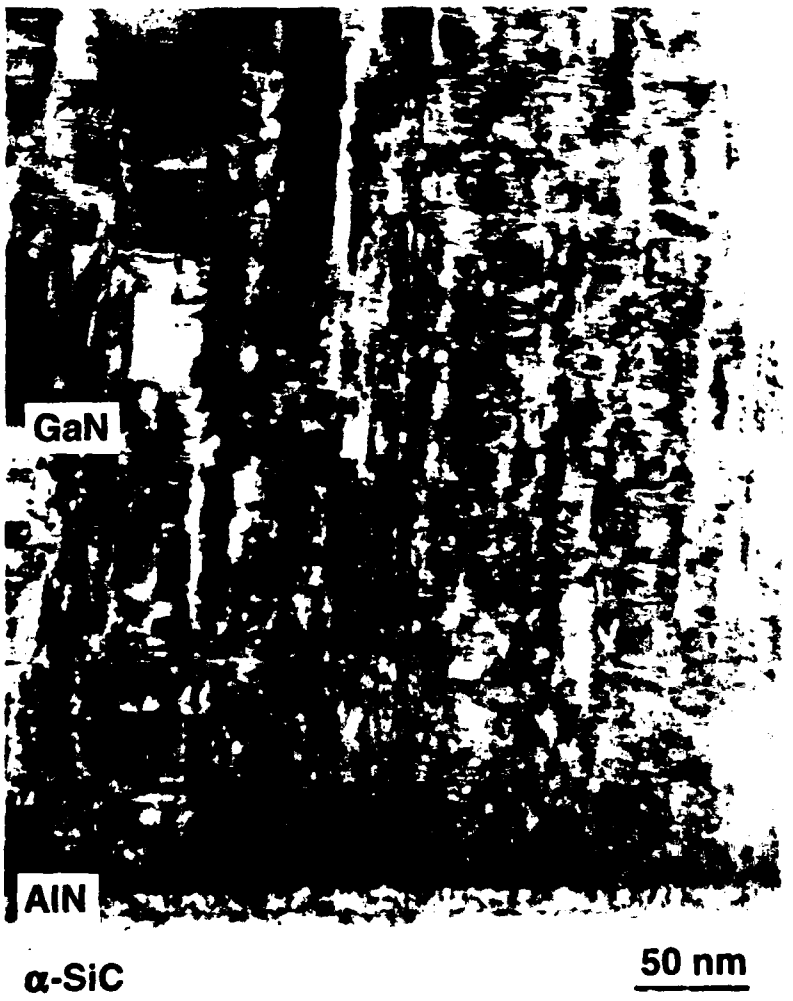

Figure 6. TEM micrograph of (a) GaN(650°C)/AlN(650°C)/α-SiC

Figure 6. Continued—TEM micrograph of (b) GaN(650°C)/α-SiC.

columnar structure by depositing the AlN buffer layer at 1100°C proceeded by the deposition of GaN at 650°C on this AlN layer. Scanning electron microscopy showed very fine surface features, however, XTEM revealed that the film again consisted of a columnar structure, as shown in Fig. 7. No apparent improvement was gained from the increase in deposition temperature of the AlN layer.

Figure 8 is a TEM micrograph of a GaN film deposited at a reduced deposition rate (five times less) and longer deposition time than the GaN film shown in Fig. 7. Again there was no apparent improvement. Furthermore, the columnar features of the film in Fig. 8 increased in number as the growth proceeded. This is similar to what was observed in the film shown in Fig. 6(a).

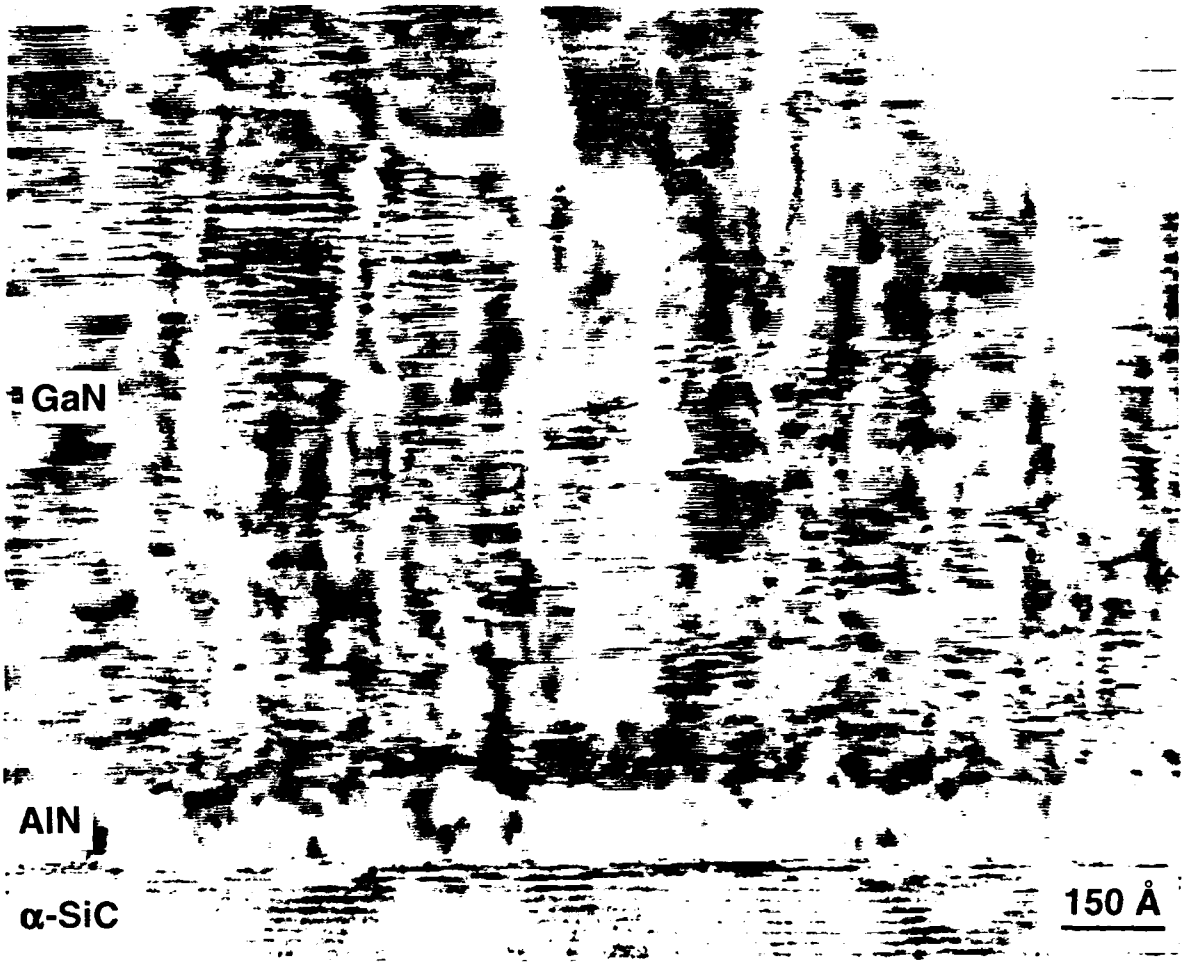

Figure 7. TEM micrograph of GaN(650°C)/AlN(1100°C)/α-SiC.

D. Discussion

There have been a lot of reports recently on the deposition of high quality single crystal GaN films [2,4,7-9]. There are two key factors realized by most MOCVD research groups, that is: i) the need for low temperature deposition of AlN or GaN buffer layers with a thickness of about 300~500Å; ii) the thickness of the GaN films needs to be 3mm or more. To date, no clear microstructural images have been presented of these high quality single crystal GaN films, especially those revealing the change in film structure with the different film thicknesses. However, several TEM pictures of the buffer layer or GaN layer near the substrate interface have been reported [9,10]. In the above section, we have presented TEM results for our GaN films deposited at various growth conditions.

In summary, we have realized that, like MOCVD, the GaN films with the buffer layer are better than the GaN films without the buffer layer. It is has been generally accepted that the buffer layer is either for stress relief or for reduction of the lattice mismatch between the

Figure 8. TEM micrograph of GaN(650°C)/AlN(1100°C)/α-SiC, the deposition rate for the GaN film was five time less than the rate for the GaN film in Figure 6.

substrate and the GaN film; the lattice mismatch between AlN/α-SiC or AlN/sapphire is less than that between GaN/α-SiC or GaN/sapphire, respectively. However, even though AlN has been used as a buffer layer between GaN and the substrate, there is still a 2.4% lattice mismatch at the GaN/AlN interface. The columnar features we have observed in the GaN films may result from the lattice mismatch. As the GaN film becomes thicker, the stress due to lattice mismatch builds up, and the columnar features become more significant. This is quite different from what MOCVD results indicate. That is, single crystal GaN film growth can be accomplished only when the films were 3mm or more in thickness.

To obtain very high quality GaN films, the columnar structure must be eliminated throughout the films. The deposition temperatures of GaN by GSMBE were much lower than

what has been used in MOCVD. However, in the low pressure deposition process of GSMBE, the deposition temperature is really limited by the desorption rate of GaN [11]. As we have shown before, when the growth temperature was increased to 900°C almost no GaN film was deposited. Therefore, we have to pursue another way to overcome the columnar structures in the films if we cannot increase the deposition rate of the GaN films dramatically by GSMBE.

As we indicated before, the lattice mismatch still exists even when epitaxial AlN was used as a buffer layer between GaN and the α-SiC substrate. In contrast to MOCVD, in which the AlN buffer layer can be amorphous or polycrystalline, we cannot deposit epitaxial GaN films by GSMBE unless the AlN buffer layer is of good crystal quality. Therefore the 2.4% lattice mismatch between AlN and GaN may play an important role in the columnar features in the GaN film. A direct way to reduce this lattice mismatch is to deposit an epitaxial buffer layer consisting of an AlN layer slowly graded to GaN on the substrate followed by the deposition of a GaN film on this graded buffer layer. However, as we found in our preliminary study, there was an abrupt change from an AlN-rich layer to a GaN-rich layer instead of a gradual graded layer. This is possibly due to the stronger attraction of Al to N than the attraction of Ga to N. Therefore, further research needs to be carried out to improve the deposition of a real graded layer.

F. Future Research Plans

As noted in the discussion part of this report, due to the limitation of GSMBE a graded $Al_xGa_{1-x}N$ solid solution buffer layer, from x=1 to x=0, would be an ideal solution for the homoepitaxy growth of GaN. Some of our future efforts will continue to involve the growth of good quality graded $Al_xGa_{1-x}N$ solid solution buffer layers. Also, we will continue our efforts to make GaN PN junction LED devices, and to study ohmic metal contacts on GaN films, reactive etching of GaN to define device structure and electroluminescence of GaN PN junction LEDs.

G. References

1. B. Goldenberg, J. D. Zook and R. J. Ulmer, Appl. Phys. Lett. **62**, 381 (1993).
2. I. Akasaki, H. Amano, N. Koide, M. Kotaki and K. Manabe, Physic B **185**, 428 (1993).
3. M. R. H. Khan, I. Akasaki, H. Amano, N. Okazaki and K. Manabe, Physic B **185**, 480 (1993).
4. S. Nakamura, M. Senoh and T. Mukai, Jpn J. Appl. Phys. **32**, L9 (1993).
5. Z. Sitar, M. J. Paisley, D. K. Smith and R. F. Davis, Rev. Sci. Instrum. **61**, 2407 (1990).
6. R. F. Davis *et al.*, R. F. Davis *et al.*, in Final Technical Report N00014-90-J-1427, P34–35 (1992).
7. M. A. Khan, J. N. Kuznia, D. T. Olson, R. Kaplan, J. Appl. Phys. **73**, 3108 (1993).
8. I. Akasaki, H. Amano, M. Sassa, H. Kato and K. Manabe, J. Crystal Growth **128**, 379 (1993).

9. J. N. Kuznia, M. A. Khan, D. T. Olson, R. Kaplan and J. Freitas, J. Appl. Phys. **73**, 4700 (1993).
10. N. Kuwano, T. Shraishi, A. Koga, K. Oki, K. Hiramatsu, H. Amano, K. Itoh and I, Akasaki, J. Crystal Growth **115**, 381 (1991).
11. N. Newman, J. Ross, and M. Rubin, Appl. Phys. Lett. **62**, 1242 (1993).

V. Distribution List

Mr. Max Yoder Office of Naval Research Electronics Division, Code: 1114SS 800 N. Quincy Street Arlington, VA 22217-5000	3
Administrative Contracting Officer Office Of Naval Research Resident Representative The Ohio State University Research Center 1960 Kenny Road Columbus, OH 43210-1063	1
Director, Naval Research Laboratory ATTN: Code 2627 Washington, DC 20375	1
Defense Technical Information Center Bldg. 5, Cameron Station Alexandria, VA 22314	12